need to be measured and incorporated into Breslauer's evaluation of nearest-neighbor interactions.[34]

Summary and Conclusions

Using chemically modified bases and standard automated oligonucleotide synthesis procedures, it is possible to prepare DNA oligomers containing internal primary amine groups that can be selectively linked to a variety of molecular labels. Successful duplex formation can occur at room temperature with oligonucleotides as short as octamers even with an internally attached label. However, the covalent attachment to an internal heterocyclic base at a position that is involved in base pairing can perturb duplex formation. The electronic absorption and emission features of the fluorescent labels used here were maintained in the labeled oligomers, but significant emission quenching occurred for both the single strand and duplex systems in some cases. This was especially true for the oligomers labeled with pyrenebutyrate: fluorescence from this label was nearly completely quenched in the duplex. This fluorophore was attached by a long and flexible linker arm to the base and thus could easily associate with or intercalate between base pairs, allowing rapid radiationless decay, quite possibly due to excited-state electron transfer to these bases. In cases where the label should remain spectroscopically observable in both single-strand and duplex forms of DNA, the covalent attachment of the label to an internal base should employ a more rigid linker arm than that used here. Sometimes the destabilizing effect of attaching a linker arm to a duplex can be overcome by label/duplex association. However, in systems that prevent such association the internally labeled duplex will probably be less stable than the corresponding unmodified duplex. This work demonstrates both the feasibility of covalent attachment of internal labels (or reporter groups) to synthetic DNA oligomers and some of the consequences of doing so. In general, attachment of an internal label is less likely to perturb duplex formation if the position of attachment is not involved in base pairing, e.g., desirable attachment sites are position 5 on the pyrimidine ring and position 8 on the purine ring. Additionally, relatively inflexible linker arms are likely to reduce label/duplex association. The latter can be constructed, for example, by use of piperazine rather than ethylenediamine in the synthesis of a modified thymidine. Other synthetic alternatives are also possible. Such inflexible linker arms could still permit intermolecular association between labels and separate duplexes. However this type of association should be infrequent at low concentrations and for hydrophilic labels.

Acknowledgment. We gratefully acknowledge the technical assistance of Raymond J. Carroll, Daniel L. Stockwell, and Lucy M. Stols (all of Amoco Technology Co.). We thank Professor Robert L. Letsinger for many helpful discussions and Doris Hung for obtaining the mass spectral data (both of Northwestern University). We thank a reviewer for helpful comments.

Registry No. $H_2N(CH_2)_3NH_2$, 109-76-2; **2**, 109082-26-0; **3**, 109082-27-1; **4**, 109082-28-2; **5**, 121351-62-0; **6**, 65505-76-2; **7**, 96203-39-3; **7** (5'-DMT derivative), 96203-40-6; **8**, 96203-41-7; **9**, 121329-87-1; **10**, 121329-88-2; GCACTCAG, 121329-89-3; GCA(C*)TCAG, 121329-90-6; GCAC(T*)CAG, 121351-63-1; GCAC(T*-biotin-LC)CAG, 121329-91-7; GCAC(T*-fluorescein)CAG, 121329-92-8; GCAC(T*-pyrenebutyrate)CAG, 121329-93-9; GCAC(T*-pyrenesulfonate)CAG, 121351-64-2; GCATCAG, 121351-65-3; GCACCAG, 121351-66-4; $H_2N(CH_2)_3NH_2$, 109-62-9; $H_2C{=}CHCOOMe$, 96-33-3; H_2NCH_2C-H_2NH_2, 107-15-3; 2'-deoxyuridine-5-(propenoic acid methyl ester), 96244-97-2; biotin, 58-85-5; fluorescein, 2321-07-5; pyrene, 129-00-0.

Multiply Charged Isoelectronic Analogues of $C_3H_3^+$: Cyclic or Open Chain?

Ming Wah Wong and Leo Radom*

Contribution from the Research School of Chemistry, Australian National University, Canberra, A.C.T. 2601, Australia. *Received March 22, 1989*

Abstract: The structures and stabilities of the isoelectronic multiply charged analogues of cyclic (cyclopropenyl cation) and open-chain (propargyl) isomers of $C_3H_3^+$, namely $C_2H_3N^{2+}$, $CH_3N_2^{3+}$, $C_2H_3O^{3+}$, $H_3N_3^{4+}$, CH_3NO^{4+}, and $C_2H_3F^{4+}$, have been investigated by ab initio molecular orbital theory. Fourth-order Møller–Plesset perturbation theory (MP4) with a triple-ζ valence plus d,p-polarization basis set (6-311G**) was employed on MP2/6-31G*-optimized geometries. In contrast to $C_3H_3^+$, for which the preferred isomer is the cyclopropenyl cation, the multiply charged analogues are found to prefer open-chain structures. The global minimum on the $C_2H_3N^{2+}$ potential energy surface is the open-chain CH_2NCH^{2+} dication (C_{2v}). Although the cyclic isomer, $\overline{CHNHCH}^{2+}$, represents a stable form of $C_2H_3N^{2+}$, it lies 35 kJ mol^{-1} higher in energy than the open structure. The CH_2NCH^{2+} ion is calculated to be thermodynamically stable with respect to proton losses and C–N bond cleavages and, hence, should be readily observable. The cyclic structure is also predicted to be a potentially observable $C_2H_3N^{2+}$ isomer. For the $CH_3N_2^{3+}$ trication, the lowest energy species corresponds to the open-chain NH_2NCH^{3+} (C_{2v}) structure. The cyclic structure, $\overline{NHCHNH}^{3+}$, lies close in energy, 39 kJ mol^{-1} above NH_2NCH^{3+}. These triply charged ions are characterized by highly exothermic fragmentation reactions. However, such dissociation reactions are inhibited by significant barriers. Thus, NH_2NCH^{3+} and $\overline{NHCHNH}^{3+}$ are predicted to be experimentally accessible in the gas phase. As in the case of $C_2H_3N^{2+}$ and $CH_3N_2^{3+}$, the $C_2H_3O^{3+}$ system also favors an open-chain structure, CH_2COH^{3+} (C_{2v}). The cyclic structure, $\overline{CHOHCH}^{3+}$, in this case represents a high-energy isomer. However, both $C_2H_3O^{3+}$ isomers are calculated to have very small barriers (less than 2 kJ mol^{-1}) associated with deprotonation reactions and, therefore, are unlikely to be observable in the gas phase. No stable equilibrium structures were found for the quadruply charged analogues of $C_3H_3^+$, namely $H_3N_3^{4+}$, CH_3NO^{4+}, and $C_2H_3F^{4+}$. The results of high-level calculations on the cyclopropenyl and propargyl cations are in very good agreement with experimental data.

The cyclopropenyl cation (**1**) is the simplest possible aromatic system with two delocalized π-electrons. This cyclic carbocation is a commonly observed species in gas-phase mass spectrometric experiments.[1] It is stable in the form of salts and also in polar

0002-7863/89/1511-6976$01.50/0

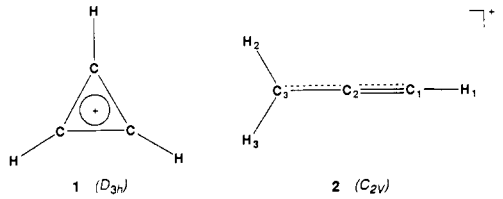

1 (D_{3h}) 2 (C_{2v})

solvents.[2] In addition, several stable substituted cyclopropenyl salts have been prepared in the laboratory.[3] The cyclopropenyl cation has a planar D_{3h} geometry.[2] The C–C bond length (1.36–1.38 Å)[3] for derivatives of **1** is even slightly shorter than that in benzene. Experimentally, the cyclic structure (**1**) is found to be more stable than the lowest energy open-chain $C_3H_3^+$ isomer, the propargyl cation (C_{2v}, **2**), by 100 kJ mol^{-1}.[1] The isoelectronic $C_2H_2N^+$ analogue also prefers a cyclic structure over an open-chain form.[4] Recently, similar preferences have also been reported for the monosubstituted systems $C_3H_2X^+$ (X = CH_3, NH_2, OH, and F).[5]

As part of our ongoing research on multiply charged cations,[6] we have been using an isoelectronic approach to search for new, potentially observable, multiply charged analogues of small, stable molecules such as CH_4,[7] N_2,[8] HCN,[9] and HCCH.[9] In this paper, we employ the same approach to investigate the possibility of a small, stable multiply charged aromatic cation. Thus, we have studied systematically the doubly, triply, and quadruply charged isoelectronic analogues of the cyclic (cyclopropenyl cation) and lowest energy open-chain (propargyl cation) isomers of $C_3H_3^+$, namely $C_2H_3N^{2+}$, $CH_3N_2^{3+}$, $C_2H_3O^{3+}$, $H_3N_3^{4+}$, CH_3NO^{4+}, and $C_2H_3F^{4+}$. Results are reported for the structures of these ions and their stabilities with respect to fragmentation. To provide an estimate of the accuracy of our computed results for the multiply charged systems, we have also calculated the structures and energies of the cyclic (**1**) and open-chain (**2**) structures of $C_3H_3^+$ with various basis sets and correlation procedures up to levels of theory significantly higher than those applied previously to these systems and compare our results with the available experimental data.

Method and Results

Using a modified version[10] of the GAUSSIAN 86 system of programs,[11] standard ab initio molecular orbital calculations[12] were carried out for $C_3H_3^+$ and its six multiply charged isoelectronic analogues.

In order to examine the effect of basis set and electron correlation on the structures of the $C_3H_3^+$ ions, we have optimized the cyclic cyclopropenyl (**1**) and open-chain propargyl (**2**) cations systematically with a sequence of basis sets of increasing size, including 6-31G,[13] 6-31G*,[14] 6-31G**,[14] and 6-311G*,[15] at Hartree–Fock (HF) and second-order Møller–Plesset perturbation theory[16] levels. To explore further the effect on relative energies, higher level single-point calculations were performed with the larger triple-ζ valence plus d,p-polarization 6-311G**, 6-311G(2d,p), and 6-311G(2d,2p) basis sets,[15,17] including electron correlation at various levels of Møller–Plesset perturbation theory (MP2, MP3, and MP4),[16,18] on the MP2/6-31G*-optimized structures.

For the multiply charged analogues of $C_3H_3^+$, geometry optimizations were carried out with the 6-31G* basis set, initially at the Hartree–Fock (HF) level and subsequently with electron correlation incorporated via second-order Møller–Plesset perturbation theory (MP2). Unless otherwise noted, geometric parameters in the text refer to the MP2/6-31G* values. Spin-restricted (RHF, RMP) calculations were used for closed-shell systems and spin-unrestricted (UHF, UMP) calculations for open-shell systems. No significant spin contamination was found for any of the open-shell species examined in this paper except for the $HCN^{\cdot+}$ ion ($\langle S^2 \rangle$ = 0.99). Harmonic vibrational frequencies were calculated at the HF/6-31G* level in order to

Table I. Optimized Geometries for the Cyclopropenyl (**1**) and Propargyl (**2**) Cations

	6-31G	6-31G*	6-31G**	MP2/6-31G*	MP2/6-311G*
		Cyclopropenyl Cation (**1**)			
r(C–C)	1.365	1.349	1.350	1.368	1.371
r(C–H)	1.065	1.072	1.072	1.083	1.082
		Propargyl Cation (**2**)			
$r(C_1–C_2)$	1.220	1.214	1.214	1.232	1.231
$r(C_2–C_3)$	1.341	1.343	1.342	1.357	1.357
$r(C_1–H_1)$	1.064	1.067	1.067	1.078	1.076
$r(C_3–H_2)$	1.077	1.078	1.079	1.091	1.090
$\angle C_2C_3H_2$	120.8	120.6	120.4	120.8	120.6

Table II. Calculated Total Energies[a] (Hartrees) and Relative Energies (kJ mol^{-1}) for the Cyclic Cyclopropenyl (**1**) and Open-Chain Propargyl (**2**) Cations

	total energy		relative energy	
	cyclic (**1**)	open (**2**)	cyclic (**1**)	open (**2**)
6-31G	114.939 06	114.913 12	0	68
6-31G*	115.007 02	114.951 10	0	147
6-31G**	115.013 29	114.956 90	0	148
MP2/6-31G*	115.363 65	115.311 30	0	137
MP2/6-311G*	115.434 78	115.385 11	0	130
HF/6-31G**[b]	115.030 45	114.975 65	0	144
MP2/6-311G**[b]	115.399 72	115.349 56	0	132
MP3/6-311G**[b]	115.420 24	115.368 23	0	137
MP4(SDQ)/6-311G**[b]	115.423 06	115.375 67	0	124
MP4/6-311G**[b]	115.440 79	115.397 16	0	115
MP4/6-311G(2d,p)[b]	115.457 00	115.415 96	0	108
MP4/6-311G(2d,2p)[b]	115.461 58	115.419 94	0	109
MP4/6-311G**[b,c]			0	108
MP4/6-311G(2d,2p)[b,c]			0	103
experiment[d]			0	100

[a] Geometries fully optimized at the level specified, unless otherwise noted. [b] MP2/6-31G*-optimized geometries. [c] Including zero-point vibrational correction. The (unscaled) zero-point vibrational energies (HF/6-31G*) for the cyclic and open structures of $C_3H_3^+$ are 127.7 and 120.7 kJ mol^{-1}, respectively. [d] From ref 1.

(1) Rosenstock, H. M.; Draxl, K.; Steiner, B. W.; Herron, J. T. *J. Phys. Chem. Ref. Data, Suppl.* **1977**, *6*.
(2) Breslow, R.; Groves, J. T. *J. Am. Chem. Soc.* **1970**, *92*, 984.
(3) (a) Sundaralingam, M.; Chwang, A. K. *Carbonium Ions* **1976**, *5*, 2427. (b) Allen, F. H. *Tetrahedron* **1982**, *38*, 645.
(4) Swanton, D. J.; Backsay, G. B.; Willett, G. D.; Hush, N. S. *THEOCHEM* **1983**, *91*, 313.
(5) Hopkinson, A. C.; Lien, M. H. *J. Am. Chem. Soc.* **1986**, *108*, 2843.
(6) For example, see: (a) Radom, L.; Gill, P. M. W.; Wong, M. W.; Nobes, R. H. *Pure Appl. Chem.* **1988**, *66*, 183. (b) Radom, L.; Gill, P. M. W.; Wong, M. W. *Int. J. Quantum Chem., Quantum Chem. Symp.* **1988**, *22*, 567. (c) Radom, L.; Wong, M. W.; Gill, P. M. W. *Adv. Mass Spectrom.*, in press.
(7) (a) Wong, M. W.; Nobes, R. H.; Radom, L. *J. Chem. Soc., Chem. Commun.* **1987**, 233. (b) Wong, M. W.; Radom, L. *Struct. Chem.*, in press. (c) Wong, M. W.; Bürgi, H. B.; Radom, L., to be submitted for publication.
(8) Wong, M. W.; Nobes, R. H.; Bouma, W. J.; Radom, L. *J. Chem. Phys.*, in press.
(9) Wong, M. W.; Nobes, R. H.; Radom, L., to be submitted for publication.
(10) (a) Nobes, R. H.; Smith, B. J.; Riggs, N. V.; Wong, M. W., unpublished results. (b) Baker, J. *J. Comput. Chem.* **1986**, *7*, 385. (c) Baker, J. *J. Comput. Chem.* **1987**, *8*, 563.
(11) Frisch, M. J.; Binkley, J. S.; Schlegel, H. B.; Raghavachari, K.; Melius, C. F.; Martin, C. L.; Stewart, J. J. P.; Bobrowicz, F. W.; Rohlfing, C. M.; Kahn, L. R.; DeFrees, D. J.; Whiteside, R. A.; Fox, D. J.; Fluder, E. M.; Pople, J. A. GAUSSIAN 86; Carnegie-Mellon University: Pittsburgh, PA, 1986.
(12) Hehre, W. J.; Radom, L.; Schleyer, P. v. R.; Pople, J. A. *Ab Initio Molecular Orbital Theory*; Wiley: New York, 1986.
(13) Hehre, W. J.; Ditchfield, R.; Pople, J. A. *J. Chem. Phys.* **1972**, *56*, 2257.
(14) Hariharan, P. C.; Pople, J. A. *Theor. Chim. Acta* **1973**, *28*, 213.
(15) Krishnan, R.; Binkley, J. S.; Seeger, R.; Pople, J. A. *J. Chem. Phys.* **1980**, *72*, 650.
(16) (a) Møller, C.; Plesset, M. S. *Phys. Rev.* **1934**, *46*, 618. (b) Pople, J. A.; Binkley, J. S.; Seeger, R. *Int. J. Quantum Chem., Quantum Chem. Symp.* **1976**, *10*, 1.
(17) Frisch, M. J.; Pople, J. A.; Binkley, J. S. *J. Chem. Phys.* **1984**, *80*, 3265.
(18) (a) Krishnan, R.; Pople, J. A. *Int. J. Quantum Chem.* **1978**, *14*, 91. (b) Krishnan, R.; Frisch, M. J.; Pople, J. A. *J. Chem. Phys.* **1980**, *72*, 4244.

Table III. Calculated Total Energies (Hartrees) and Zero-Point Vibrational Energies[a] (ZPVE, kJ mol^{-1}) for $C_3H_3^+$, $C_2H_3N^{2+}$, $CH_3N_2^{3+}$, and $C_2H_3O^{3+}$ Cations and Related Species

species	state	symmetry	N_i[b]	total energy HF/6-31G*	total energy MP2/6-31G*	total energy MP4/6-311G**[c]	ZPVE
$\overline{CHCHCH}^+$ (1)	$^1A_1$	D_{3h}	0	−115.007 02	−115.363 65	−115.440 79	127.7
CH_2CCH^+ (2)	$^1A_1$	C_{2v}	0	−114.951 10	−115.311 30	−115.397 16	120.7
$CHCHCH^+$ (3)	^1A	C_1	0	−114.820 59	−115.149 12	−115.246 40	106.6
TS: 3 → 2 (4)	^1A	C_1	1	−114.808 98	−115.141 47	−115.235 34	102.1
TS: 3 → 1 (5)	^1A	C_1	1	−114.812 34	−115.142 06	−115.241 75	107.0
CH_2NCH^{2+} (6)	$^1A_1$	C_{2v}	0	−131.019 14	−131.388 81	−131.476 84	121.0
CH_2CNH^{2+} (7)	$^1A_1$	C_{2v}	0	−130.999 57	−131.382 50	−131.470 41	120.2
NH_2CCH^{2+} (8)	$^1A_1$	C_{2v}	0	−130.946 85	−131.330 72	−131.427 70	121.1
$\overline{CHNHCH}^{2+}$ (9)	$^1A_1$	C_{2v}	0	−131.000 54	−131.379 64	−131.464 91	125.1
CH_2NC^+	$^1A_1$	C_{2v}	0	−130.954 25	−131.325 17	−131.412 28	90.4
$HCNCH^+$	$^1A'$	C_s	0	−130.898 20	−131.280 69	−131.368 84	83.0
$\overline{CHNCH}^+$	$^1A_1$	C_{2v}	0	−130.975 08	−131.357 83	−131.436 53	94.6
$\overline{CHCNH}^+$	$^1A'$	C_s	0	−130.911 02	−131.295 25	−131.381 35	93.1
CH_2N^+	$^1A_1$	C_{2v}	0	−93.055 70	−93.307 86	−93.383 12	66.2
$HCN^{\cdot+}$	$^2\Sigma^+$	$C_{\infty v}$	0	−92.420 77	−92.644 22	−92.705 16	41.7
$CH_2^{\cdot+}$	$^2A_1$	C_{2v}	0	−38.566 19	−38.639 19	−38.678 77	46.8
CH^+	$^1\Sigma^+$	$C_{\infty v}$	0	−37.895 54	−37.965 26	−38.004 03	19.1
NH_2NCH^{3+} (10)	$^1A_1$	C_{2v}	0	−146.609 05	−147.019 40	−147.123 38	110.5
NH_2CNH^{3+} (11)	$^1A_1$	C_{2v}	0	−146.581 52	−147.009 02	−147.118 51	101.5
$\overline{NHCHNH}^{3+}$ (12)	$^1A_1$	C_{2v}	0	−146.594 04	−147.011 70	−147.108 14	109.2
TS: 10 → NH_2NC^{2+} + H^+ (16)	$^1A_1$	C_{2v}	1	−146.569 32	−146.984 27	−147.085 19	93.1
TS: 10 → H^+ + $HNNCH^{2+}$ (17)	$^1A'$	C_s	1	−146.569 85	−146.981 92	−147.080 33	89.9
TS: 12 → H^+ + $\overline{NHCNH}^{2+}$ (18)	$^1A_1$	C_{2v}	1	−146.546 36	−146.968 98	−147.062 53	90.0
TS: 12 → H^+ + $\overline{NHNCH}^{2+}$ (19)	$^1A'$	C_s	1	−146.572 85	−146.994 54	−147.085 93	93.0
NH_2NC^{2+}	$^1A_1$	C_{2v}	0	−146.831 98	−147.243 13	−147.345 80	88.7
$HNNCH^{2+}$	$^1A'$	C_s	0	−146.860 02	−147.264 46	−147.364 24	82.6
$\overline{NHCNH}^{2+}$	$^1A_1$	C_{2v}	0	−146.815 12	−147.237 98	−147.335 15	86.8
$\overline{NHNCH}^{2+}$	$^1A'$	C_s	0	−146.876 82	−147.292 79	−147.384 62	90.5
NH_2N^{2+}	$^1A_1$	C_{2v}	0	−108.942 66	−109.240 15	−109.323 59	59.6
$NH_2^{\cdot 2+}$	$^2\Pi_u$	$D_{\infty h}$	0	−54.320 12	−54.403 42	−54.456 81	38.1
CH_2COH^{3+} (13)	$^1A_1$	C_{2v}	0	−150.482 11	−150.862 62	−150.972 08	101.3
OH_2CCH^{3+} (14)	$^1A_1$	C_{2v}	0	−150.390 43	−150.771 09	−150.884 65	103.4
$\overline{CHOHCH}^{3+}$ (15)	$^1A_1$	C_{2v}	0	−150.391 13	−150.778 76	−150.882 66	100.7
TS: 13 → H^+ + $HCCOH^{2+}$ (20)	$^1A'$	C_s	1	−150.427 17	−150.812 67	−150.920 38	76.2
TS: 13 → CH_2^{2+} + HOC^+ (21)	$^1A_1$	C_{2v}	1	−150.471 59	−150.832 83	−150.945 68	95.4
TS: 13 → CH_2CO^{2+} + H^+ (22)	$^1A_1$	C_{2v}	1	−150.473 82	−150.861 10	−150.967 18	89.0
TS: 15 → H^+ + $\overline{CHOCH}^{2+}$ (23)	$^1A_1$	C_{2v}	1	−150.385 32	−150.778 22	−150.878 93	91.4
CH_2CO^{2+}	$^1A_1$	C_{2v}	0	−150.754 26	−151.154 36	−151.253 85	87.7
$HCCOH^{2+}$	$^1A'$	C_s	0	−150.669 25	−151.061 94	−151.169 72	80.2
$\overline{CHOCH}^{2+}$	$^1A_1$	C_{2v}	0	−150.709 95	−151.108 82	−150.203 89	88.7
CCH_2^{2+}	$^3B_1$	C_{2v}	0	−75.721 78	−75.868 42	−75.920 85	63.3
HOC^+	$^1\Sigma^+$	$C_{\infty v}$	0	−112.914 39	−113.191 19	−113.270 19	36.6
CH_2^{2+}	$^1\Sigma_g^+$	$D_{\infty h}$	0	−37.800 37	−37.865 02	−37.900 97	47.2
OH^+	$^3\Sigma^-$	$C_{\infty v}$	0	−74.968 75	−75.067 77	−75.132 45	20.1

[a] HF/6-31G* values. [b] Number of imaginary frequencies. [c] MP2/6-31G*-optimized structures.

characterize stationary points as minima (representing equilibrium structures) or saddle points (representing transition structures) and to determine zero-point vibrational energies (ZPVEs). The directly calculated ZPVEs were scaled by a factor of 0.9[19] to allow for the overestimation of vibrational frequencies at this level of theory. Improved relative energies were obtained from full fourth-order Møller–Plesset (MP4) calculations with the 6-311G** basis set based on the MP2/6-31G*-optimized geometries. Our best relative energies correspond to MP4/6-311G**//MP2/6-31G* values with zero-point vibrational corrections. Unless otherwise noted, these are the values given in the text.

Optimized geometries for the cyclopropenyl and propargyl cations are shown in Table I and corresponding total and relative energies in Table II. All the tetracation analogues of $C_3H_3^+$, namely $H_3N_3^{4+}$, CH_3NO^{4+}, and $C_2H_3F^{4+}$, are found to be unstable species and dissociate without a barrier to more stable fragments upon geometry optimization. For the remaining dications, trications, and $C_3H_3^+$ itself, the calculated total energies and relative energies are summarized in Tables III and IV, respectively, and the optimized (MP2/6-31G*) structures displayed within the text. Bond lengths and bond angles throughout this paper are in angstroms and degrees, respectively. The frozen-core approximation was employed in all the Møller–Plesset calculations except the MP2 optimizations.

Discussion

$C_3H_3^+$ Ion. Structural and Energy Comparisons. The $C_3H_3^+$ ion has already been examined in great detail by numerous ab initio studies.[20,21] We consider here only the structures and

(19) Pople, J. A.; Schlegel, H. B.; Krishnan, R.; DeFrees, D. J.; Binkley, J. S.; Frisch, M. J.; Whiteside, R. A.; Hout, R. F.; Hehre, W. J. *Int. J. Quantum Chem., Quantum Chem. Symp.* **1981**, *15*, 269.

(20) (a) Radom, L.; Hariharan, P. C.; Pople, J. A.; Schleyer, P. v. R. *J. Am. Chem. Soc.* **1976**, *98*, 10. (b) Takada, T.; Ohno, K. *Bull. Chem. Soc. Jpn.* **1979**, *52*, 334. (c) Radom, L.; Poppinger, D.; Haddon, R. C. *Carbonium Ions* **1976**, *5*, 2303. (d) Norden, T. D.; Staley, S. W.; Taylor, W. H.; Harmony, M. D. *J. Am. Chem. Soc.* **1986**, *108*, 7912.

(21) Raghavachari, K.; Whiteside, R. A.; Pople, J. A.; Schleyer, P. v. R. *J. Am. Chem. Soc.* **1981**, *103*, 5649.

Table IV. Calculated Relative Energies[a] (kJ mol^{-1}) for Equilibrium and Transition Structures and Fragmentation Products of $C_3H_3^+$, $C_2H_3N^{2+}$, $CH_3N_2^{3+}$, and $C_2H_3O^{3+}$

species	HF/ 6-31G*	MP2/ 6-31G*	MP4/ 6-311G**	MP4/ 6-311G**[b]
CH_2CCH^+ (**2**)	0	0	0	0
$\overline{CHCHCH}^+$ (**1**)	−147	−137	−115	−108
$CHCHCH^+$ (**3**)	343	426	396	383
TS: **3** → **2** (**4**)	373	446	425	408
TS: **3** → **1** (**5**)	364	444	408	396
CH_2NCH^{2+} (**6**)	0	0	0	0
CH_2CNH^{2+} (**7**)	51	17	17	16
NH_2CCH^{2+} (**8**)	190	153	129	129
$\overline{CHNHCH}^{2+}$ (**9**)	49	24	31	35
$CH_2NC^+ + H^+$	170	167	170	142
$HCNCH^+ + H^+$	318	284	284	249
$\overline{CHNCH}^+ + H^+$	117	81	106	82
$\overline{CHCNH}^+ + H^+$	284	246	251	226
$CH_2^{\cdot+} + HCN^{\cdot+}$	85	277	244	215
$CH_2N^+ + CH^+$	178	304	236	203
NH_2NCH^{3+} (**10**)	0	0	0	0
NH_2CNH^{3+} (**11**)	72	27	13	5
$\overline{NHCHNH}^{3+}$ (**12**)	39	20	40	39
TS: **10** → $NH_2NC^{2+} + H^+$ (**16**)	104	92	100	85
TS: **10** → $H^+ + HNNCH^{2+}$ (**17**)	103	98	113	95
TS: **12** → $\overline{NHCNH}^{2+} + H^+$ (**18**)	165	132	160	142
TS: **12** → $\overline{NHNCH}^{2+} + H^+$ (**19**)	95	65	98	83
$NH_2NC^{2+} + H^+$	−585	−587	−584	−604
$HNNCH^{2+} + H^+$	−659	−643	−632	−658
$\overline{NHCNH}^{2+} + H^+$	−541	−574	−556	−577
$\overline{NHNCH}^{2+} + H^+$	−703	−718	−686	−704
$NH_2^{\cdot 2+} + HCN^{\cdot+}$	−346	−74	−101	−129
$NH_2N^{2+} + CH^+$	−602	−488	−536	−565
CH_2COH^{3+} (**13**)	0	0	0	0
OH_2CCH^{3+} (**14**)	241	240	230	231
$\overline{CHOHCH}^{3+}$ (**15**)	239	220	235	234
TS: **13** → $H^+ + HCCOH^{2+}$ (**20**)	144	131	136	113
TS: **13** → $CH_2^{2+} + HOC^+$ (**21**)	28	78	69	64
TS: **13** → $CH_2CO^{2+} + H^+$ (**22**)	22	4	13	2
TS: **15** → $\overline{CHOCH}^{2+} + H^+$ (**23**)	254	222	246	235
$CH_2CO^{2+} + H^+$	−715	−766	−740	−752
$HCCOH^{2+} + H^+$	−491	−523	−519	−538
$\overline{CHOCH}^{2+} + H^+$	−598	−646	−609	−620
$CH_2^{2+} + HOC^+$	−611	−508	−523	−539
$CCH_2^{2+} + OH^+$	−547	−193	−213	−229

[a] Based on calculated total energies from Table III. [b] Including zero-point vibrational correction.

energies of the cyclic cyclopropenyl (**1**) and open-chain propargyl (**2**) cations to establish the likely accuracy of the calculated results for the multiply charged species and to provide a benchmark assessment of the various levels of theory for structural and energy predictions. In addition, we have examined the reaction profile for the rearrangement of **2** to **1**.

Both the cyclic (**1**) and open-chain (**2**) structures of $C_3H_3^+$ have been optimized with five different levels of theory, including HF/6-31G, HF/6-31G*, HF/6-31G**, MP2/6-31G*, and MP2/6-311G* levels. From Table I, it can be seen that the variation in geometrical parameters calculated at various levels of theory for **1** and **2** is generally small. The largest effect appears to be associated with the incorporation of electron correlation (HF/6-31G* → MP2/6-31G*). The changes are, however, systematic: the calculated C–C and C–H bond lengths at the MP2 level are uniformly longer than the corresponding values at the Hartree–Fock level. Concerning the effect of basis set, the only significant changes occur in going from 6-31G to 6-31G*, i.e., inclusion of d-polarization functions on carbon atoms. The effect of including p-polarization functions on hydrogen atoms (6-31G* → 6-31G**) and increasing the basis set from double-ζ valence to triple-ζ valence (6-31G* → 6-311G*) is very small. The only experimental data available for the structures of the $C_3H_3^+$ ions come from X-ray crystallographic studies of derivatives of the cyclopropenyl cation (**1**).[3] These experiments yielded C–C bond lengths in the range 1.36–1.38 Å for several derivatives of **1**, in good agreement with the present MP2 results. Hence, we believe that the MP2/6-31G* level should be suitably reliable for structural predictions for the multiply charged systems.

The calculated energy difference between the cyclic (**1**) and open-chain (**2**) structures (Table II) is quite dependent on the theoretical level employed. At the HF/6-31G level, **1** is more stable than **2** by 68 kJ mol^{-1}; this is dramatically increased to 147 kJ mol^{-1} when d-polarization functions are included on carbon (HF/6-31G*). This is because d functions are particularly important for an adequate description of small ring systems.[12,14] Inclusion of p-polarization functions on hydrogen (6-31G* → 6-31G**) has very little effect on the relative energy. When electron correlation is incorporated at second order (HF → MP2), the relative energies are reduced by about 10 kJ mol^{-1}. A further reduction is noted in going from MP2 to partial fourth order (MP4(SDQ)). The best relative energy reported previously is that of Raghavachari et al.[21] who obtained an energy difference between **1** and **2** of 130 kJ mol^{-1} at the MP4(SDQ)/6-31G**//HF/6-31G* level, compared with the experimental value of 100 kJ mol^{-1}.[1] We obtain a similar result in the present study at the MP4(SDQ)/6-311G**//MP2/6-31G* level (124 kJ mol^{-1}). However, inclusion of triple substitutions in the MP4 calculations, i.e., full fourth order (MP4), improves the relative energy by 9 kJ mol^{-1}. Further improvement (by 6 kJ mol^{-1}) is obtained by expanding the basis set from one set of d functions to two sets (6-311G** → 6-311G(2d,p)). MP4 calculations with our largest basis set, MP4/6-311G(2d,2p)//MP2/6-31G*, give an energy difference between **1** and **2** of 109 kJ mol^{-1}. Zero-point vibrational correction leads to our final and best value of 103 kJ mol^{-1}, in excellent agreement with the experimental result (100 kJ mol^{-1}). The present MP4/6-311G**//MP2/6-31G* + ZPVE value (108 kJ mol^{-1}) also agrees well with experiment. Hence, this level of theory is used for our highest level energy comparisons in the remainder of this paper.

The reaction profile for the rearrangement of the propargyl cation (**2**) to the cyclopropenyl cation (**1**) has been studied recently by Hopkinson and Lien[5] at the HF/6-31G* level. Their calculations predicted that the conversion of **2** to **1** requires a substantial barrier of 437 kJ mol^{-1}. Moreover, they found a metastable intermediate on the reaction profile. We have reexamined the rearrangement connecting **2** and **1** at levels of theory significantly higher than those used previously,[5] including full geometry optimization at a correlated level of theory. In agreement with Hopkinson and Lien,[5] we also find a stable intermediate (**3**, C_1;

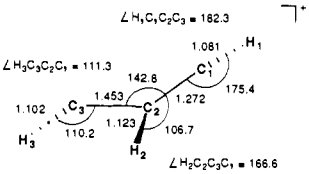

3 (C_1)

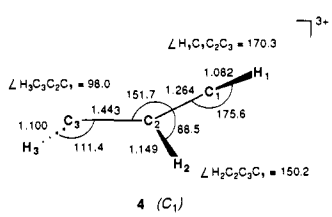

4 (C_1)

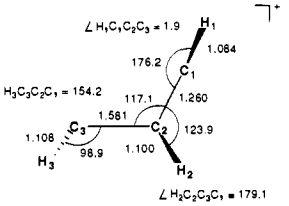

5 (C_1)

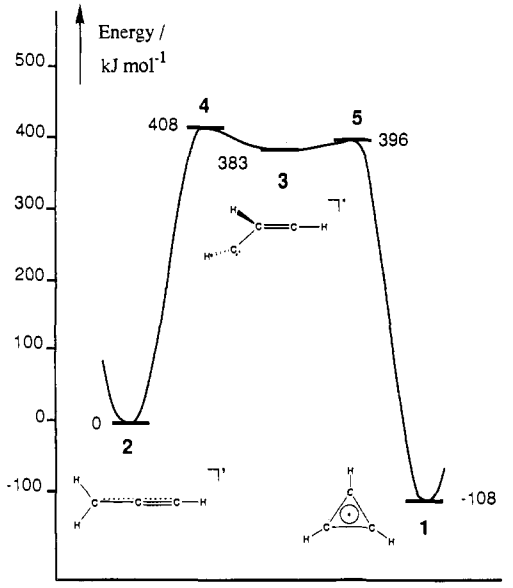

Figure 1. Reaction profile (MP4/6-311G**//MP2/6-31G* + ZPVE) for rearrangement of the propargyl cation (**2**) to the cyclopropenyl cation (**1**).

as confirmed by frequency calculations), which resembles a carbene at one terminal carbon and a vinyl cation at the other. It lies very high in energy, 383 kJ mol^{-1} above the propargyl cation (**2**). Rearrangement of this species (**3**) to the open-chain isomer (**2**), via transition structure **4**, is associated with a barrier of 25 kJ mol^{-1}, while conversion of **3** to the cyclic structure (**1**), via transition structure **5**, requires a smaller barrier of 13 kJ mol^{-1}. Our higher level calculations confirm the previous findings[5] that the rearrangement reaction **2** → **1** is impeded by a large activation barrier (408 kJ mol^{-1}). A schematic energy profile summarizing our results for the rearrangement of **2** to **1** is displayed in Figure 1.

Relative Energies: Cyclic versus Open Chain

As mentioned in the introduction, the isoelectronic monocation analogue, $C_2H_2N^+$, as well as the monosubstituted derivatives, $C_2H_3X^+$ (X = CH_3, NH_2, OH, and F), of $C_3H_3^+$ are found to prefer cyclic structures over open-chain forms. It is intriguing to ask whether the multiply charged analogues of $C_3H_3^+$ also favor cyclic aromatic structures.

$C_2H_3N^{2+}$. Three possible structures corresponding to the propargyl cation (**2**) were considered, namely CH_2NCH^{2+} (C_{2v}, **6**), CH_2CNH^{2+} (C_{2v}, **7**), and NH_2CCH^{2+} (C_{2v}, **8**). The most

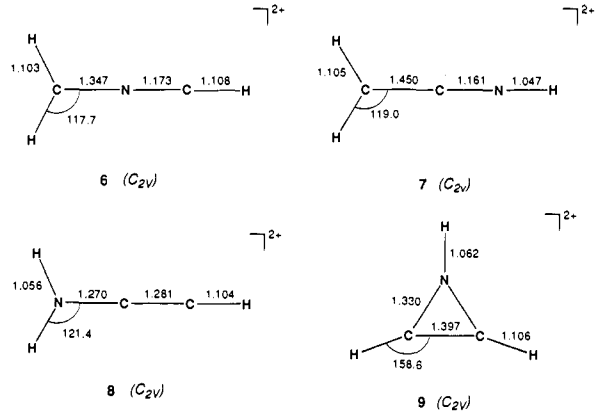

stable of these is CH_2NCH^{2+} (**6**). **7** and **8** are 16 and 129 kJ mol^{-1}, respectively, higher in energy than **6**. Although the cyclic isomer, $\overline{CHNHCH}^{2+}$ (C_{2v}, **9**), is found to be stable, it lies 35 kJ mol^{-1} above the most stable open-chain structure (**6**). We have also examined other open-chain structures CH_3CN^{2+}, CH_3NC^{2+}, and NH_3CC^{2+}; preliminary calculations indicated, however, that they are either high-energy or unstable species, and they were not investigated further.

$CH_3N_2^{3+}$. As in the case of $C_2H_3N^{2+}$, $CH_3N_2^{3+}$ also favors an open-chain structure. The lowest energy isomer of $CH_3N_2^{3+}$ corresponds to NH_2NCH^{3+} (C_{2v}, **10**). The NH_2CNH^{3+} (C_{2v},

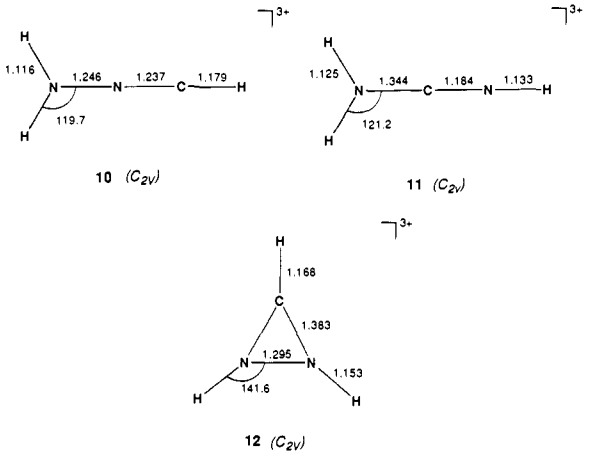

11) isomer lies close in energy, only 5 kJ mol^{-1} above **10**. Note the large change in relative energy between **11** and **10** (Table IV) in going from the HF/6-31G* (72 kJ mol^{-1}) to the MP2/6-31G* (27 kJ mol^{-1}) level. This shows the importance of electron correlation in providing a satisfactory description of NH_2CNH^{3+} (**11**). The cyclic structure of $C_2H_3N^{3+}$ (C_{2v}, **12**) is predicted to lie 39 kJ mol^{-1} above **10**. No stable equilibrium structure was found for a possible CH_2NNH^{3+} isomer.

$C_2H_3O^{3+}$. On the $C_2H_3O^{3+}$ potential energy surface, we have examined four possible isomers, CH_2COH^{3+} (C_{2v}, **13**), OH_2CCH^{3+}

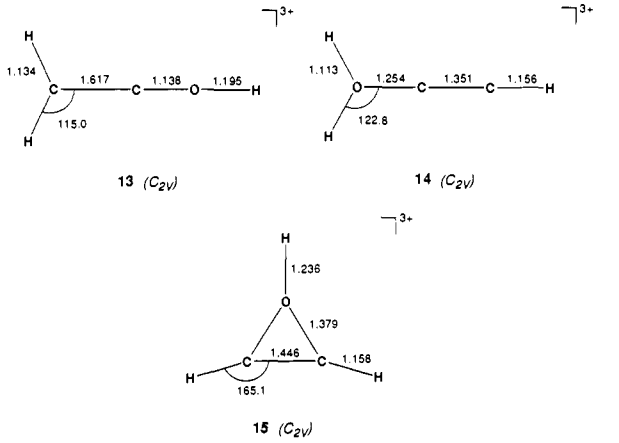

(C_{2v}, **14**), $\overline{CHOHCH}^{3+}$ (C_{2v}, **15**), and CH_2OCH^{3+}. As with $C_2H_3N^{2+}$ and $CH_3N_2^{3+}$, an open-chain structure, CH_2COH^{3+} (**13**), represents the most stable isomer. The cyclic structure (**15**) in this case represents a high-energy isomer (234 kJ mol^{-1} above **13**). The other open-chain form OH_2CCH^{3+} (**14**) also lies high in energy (231 kJ mol^{-1} above **13**). The CH_2OCH^{3+} isomer is found not to be stable, spontaneously fragmenting to CH_2^{2+} + HCO^+ upon optimization.

In summary, we find that, in contrast to the $C_3H_3^+$ system, the multiply charged analogues $C_2H_3N^{2+}$, $CH_3N_2^{3+}$, and $C_2H_3O^{3+}$ prefer open-chain structures. These preferences can be understood in terms of the strong coulomb repulsion between the positively charged hydrogen atoms in the multiply charged species;[22] i.e., electrostatically, the charge distributions in the open-chain structures are generally more favorable than those in the cyclic structures. Nevertheless, for the $C_2H_3N^{2+}$ and $CH_3N_2^{3+}$ systems, the cyclic structures lie close in energy to the lowest energy

(22) Schleyer, P. v. R. *Prepr.–Am. Chem. Soc. Div. Pet. Chem.* **1983**, *28*, 413.

Table V. Calculated (MP2/6-31G*) and Experimental Bond Lengths for Prototype Systems[a]

bond	MP2/ 6-31G*	exptl	bond	MP2/ 6-31G*	exptl
H_3C-H	1.090	1.092	$HC\equiv N$	1.177	1.153
H_2N-H	1.017	1.012	H_3C-OH	1.424	1.421
$HO-H$	0.969	0.958	$H_2C=O$	1.221	1.208
H_3C-CH_3	1.527	1.531	$C\equiv O$	1.151	1.128
$H_2C=CH_2$	1.336	1.339	H_2N-NH_2	1.439	1.449
$HC\equiv CH$	1.218	1.203	$HN=NH$	1.267	1.252
H_3C-NH_2	1.465	1.471	$N\equiv N$	1.131	1.098
$H_2C=NH$	1.282	1.273			

[a] From ref 12.

open-chain isomers. The cyclic structure of $C_2H_3O^{3+}$, on the other hand, represents a high-energy species.

Structural Features

The stable species examined in this paper display interesting structural features that warrant further discussion. For comparison purposes, MP2/6-31G* and experimental bond lengths for prototype systems[12] are shown in Table V.

X–H (X = C, N, and O) Bond Lengths. As pointed out previously,[6,22,23] bonds to hydrogen in doubly charged ions are generally long compared with those in neutral molecules and monocations. This may be attributed to the electropositive nature of hydrogen and strong coulomb repulsion in dications. It might be expected that the stronger coulomb repulsion in triply charged species should result in even longer X–H bond lengths. Indeed, the C–H and N–H bonds of the triply charged species studied here are about 0.05 Å longer than the corresponding bonds in doubly charged ions. The oxygen-containing trications **13** and **15** display particularly long O–H bonds, about 0.20–0.25 Å longer than normal O–H bonds. Mulliken population analysis indicates that the hydrogen atoms of these O–H bonds have charges close to unity (+0.84 and +0.83, respectively).

Open-Chain Structures. The open-chain isomers considered here are found to have skeletal structures, which generally lie between extremes that may be described as allenic and acetylenic. For example, of the three isomeric forms of $C_2H_3N^{2+}$, namely CH_2NCH^{2+} (**6**), CH_2CNH^{2+} (**7**), and NH_2CCH^{2+} (**8**), **7** has an acetylenic-type structure, **8** displays an allenic-type skeleton, while **6** has a structure somewhere in between.

To understand these structural differences in the open-chain isomers, we begin by examining the structure of the parent propargyl cation (**2**). This ion can be represented by two principal resonance structures: acetylenic (**2a**) and allenic (**2b**), formally

2a **2b**

derived by removing a hydride ion from propyne and allene, respectively. Since propyne and allene have similar energies, the propargyl cation (**2**) has comparable contributions from each of **2a** and **2b**, and the resultant structure is intermediate between that of propyne and allene. Indeed, the calculated C_1-C_2 bond distance (1.232 Å) in **2** is intermediate between that of a double and a triple bond, while the C_2-C_3 bond distance (1.357 Å) is intermediate between that of a single and a double bond.

For multiply charged species, coulomb repulsion is crucial in determining the stability of a particular resonance structure. Thus, we find that the relative importance of various contributing structures of the resonance hybrids can be assessed by a simple consideration of their charge distributions. *Resonance structures with delocalized charges are more favorable than structures with localized charges.* This is a restatement of Pauling's electroneutrality rule.[24] We illustrate this approach in a rationalization of the different structures of the three open-chain isomers of $C_2H_3N^{2+}$ (**6–8**). For CH_2NCH^{2+} (**6**), neither the acetylenic (**6a**)

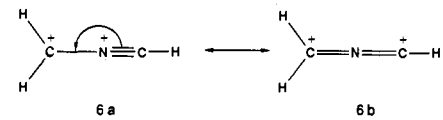

6a **6b**

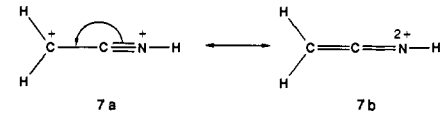

7a **7b**

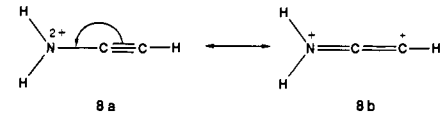

8a **8b**

nor the allenic (**6b**) resonance structures are particularly unfavorable and, therefore, the resulting structure is intermediate between **6a** and **6b**; i.e., **6** has a propargyl-like structure. On the other hand, the charge-separated acetylenic structure (**7a**) is more favorable than the charge-localized allenic structure (**7b**) in CH_2CNH^{2+} (**7**). Thus, **7** has a preferred acetylenic-type structure. Likewise, the greater contribution of the charge-separated structure (**8b**) leads to an allenic-type N–C–C skeleton in NH_2CCH^{2+} (**8**).

The structural features of other open-chain structures (**10**, **11**, and **14**) can be similarly rationalized by the above approach. Moreover, the unusual structure of CH_2COH^{3+} (**13**) can also be nicely rationalized in electrostatic terms by considering an additional resonance structure. Examination of the acetylenic (**13a**) and allenic (**13b**) structures for **13** shows clearly that electron redistribution in the direction of **13b** should be unfavorable. In

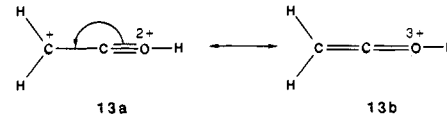

13a **13b**

this case, there is some electron redistribution in the *opposite* direction, leading to the additional no-bond resonance structure (**13c**), which resembles a sum of two fragments (CH_2^{2+} + HOC^+).

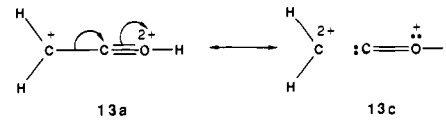

13a **13c**

Structures **13a** and **13c** are comparable from an electrostatic point of view leading to substantial contributions in the resulting resonance hybrid. As a consequence, CH_2COH^{3+} has a rather elongated C–C bond (1.617 Å), even longer than that of a typical C–C single bond (1.527 Å in ethane at MP2/6-31G*), and a short C–O bond (1.138 Å), comparable to the C–O triple bond length (1.151 at MP2/6-31G*)[12] of carbon monoxide.

Cyclic Structures. As for the open-chain structures, one can readily rationalize the bond lengths in the cyclic isomers, namely $\overline{CHNHCH}^{2+}$ (**9**), $\overline{NHCHNH}^{3+}$ (**12**), and $\overline{CHOHCH}^{3+}$ (**15**), by considering the contributions of the various possible resonance structures in each case. For example, the cyclic structure of $C_2H_3N^{2+}$ (**9**) can be represented by three resonance structures:

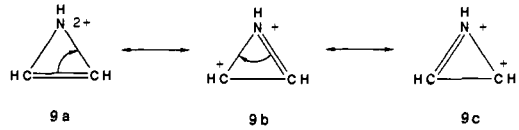

9a **9b** **9c**

Both **9b** and **9c** are more favorable (electrostatically) than **9a** and therefore have greater contributions to the resonance hybrid. As

(23) Koch, W.; Schwarz, H. In *Structure/Reactivity and Thermochemistry of Ions*; Ausloos, P., Lias, S. G., Eds.; Reidel: Dordrecht, The Netherlands, 1987.

(24) Pauling, L. *J. Chem. Soc.* **1948**, 1461.

a result, the C–C bond is lengthened and the C–N bond is shortened.

Stability Predictions

In order to assess whether the multiply charged species are likely to be experimentally observable, it is necessary to examine the thermodynamic and kinetic stabilities of these ions. We have restricted our attention to stabilities with respect to simple bond cleavage reactions on the basis that additional barriers are likely to be associated with rearrangement processes.

$C_2H_3N^{2+}$. We have examined four possible fragmentation processes for the CH_2NCH^{2+} dication (**6**). Deprotonation of **6** can lead to $CH_2NC^+ + H^+$ or $HCNCH^+ + H^+$. Both processes are calculated to be endothermic (by 142 and 249 kJ mol^{-1}, respectively) and associated with large fragmentation barriers. Likewise, the fragmentation processes giving $CH_2^{\cdot+} + HCN^{\cdot+}$ and $CH_2N^+ + CH^+$ are also found to be endothermic (by 215 and 203 kJ mol^{-1}, respectively). Thus, CH_2NCH^{2+} is predicted to lie in a deep potential well and should be readily observable. How about the cyclic isomer of $C_2H_3N^{2+}$ (**9**)? As in the case of the open-chain isomer (**6**), the cyclic structure (**9**) is also predicted to be thermodynamically stable with respect to proton losses. Deprotonation reactions of **9** to give $H^+ + \overline{CHNCH}^+$ or $H^+ + \overline{CHCNH}^+$ are calculated to be endothermic by 47 and 191 kJ mol^{-1}, respectively. Ring-opening reactions of **9**, which would remove any aromatic stabilization, are expected to have sizable activation barriers, by analogy with $C_3H_3^+$ (see above). Hence, the cyclic structure (**9**) is also predicted to be a potentially observable $C_2H_3N^{2+}$ isomer.

The heat of formation ($\Delta H_f°$) of the CH_2NCH^{2+} dication (**6**) can be estimated from the energy (215 kJ mol^{-1}) of the reaction

$$CH_2NCH^{2+} \rightarrow CH_2^{\cdot+} + HCN^{\cdot+}$$

Combining this with the experimental heats of formation[1] for $CH_2^{\cdot+}$ (1398 kJ mol^{-1}) and $HCN^{\cdot+}$ (1447 kJ mol^{-1}) gives a heat of formation of 2630 kJ mol^{-1} for CH_2NCH^{2+}. Adding the energy difference between **6** and **9** (35 kJ mol^{-1}) to the calculated heat of formation of **6** leads to a prediction for the heat of formation for the cyclic structure (**9**) of 2665 kJ mol^{-1}.

$CH_3N_2^{3+}$. In marked contrast to the $C_2H_3N^{2+}$ dications, fragmentation reactions of the triply charged ion NH_2NCH^{3+} (**10**) are highly exothermic. Deprotonation of **10** to $NH_2NC^{2+} + H^+$ or $H^+ + HNNCH^{2+}$ is exothermic by 604 and 658 kJ mol^{-1}, respectively. Both processes are, however, inhibited by significant barriers of 85 and 95 kJ mol^{-1}, respectively (via transition structures **16** and **17**). Fission of the C–N bonds to give $NH_2^{\cdot 2+}$

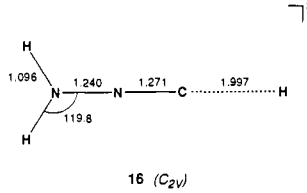

16 (C_{2v})

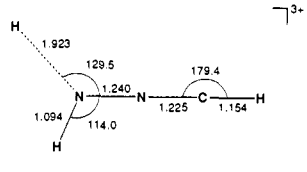

17 (C_s)

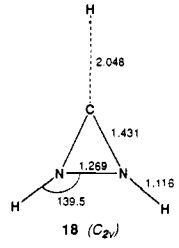

18 (C_{2v})

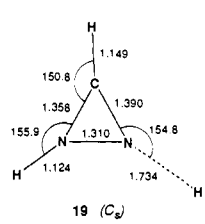

19 (C_s)

+ $HCN^{\cdot+}$ or $NH_2N^{2+} + CH^+$ is also calculated to be exothermic (by 129 and 565 kJ mol^{-1}, respectively). However, such dissociations, which require the breaking of strong multiple bonds, are also expected to require substantial activation energy. Therefore, the triply charged NH_2NCH^{3+} ion is predicted to be experimentally accessible in the gas phase, perhaps through charge-stripping of the corresponding dication. For the cyclic structure (**12**), the fragmentations to $H^+ + \overline{NHCNH}^{2+}$ or $H^+ + \overline{NHNCH}^{2+}$ are exothermic by 616 and 743 kJ mol^{-1}, respectively. However, such dissociations (via transition structures **18** and **19**) require sizable activation barriers (103 and 44 kJ mol^{-1}, respectively). Hence, **12** is also predicted to be a potentially observable species.

$C_2H_3O^{3+}$. As with $CH_3N_2^{3+}$, proton losses and C–C and C–O cleavages of CH_2COH^{3+} (**13**) are extremely exothermic processes (Table IV). Dissociation reactions of **13** to $HCCOH^{2+} + H^+$ and $CH_2^{2+} + HOC^+$ (via transition structures **20** and **21**, respectively) require significant activation energies of 113 and 64 kJ mol^{-1}, respectively. On the other hand, a small barrier of just 2 kJ mol^{-1} is associated with the deprotonation reaction $CH_2COH^{3+} \rightarrow CH_2CO^{2+} + H^+$. For the cyclic isomer (**15**), the very long O–H bond suggests that its cleavage should also be relatively easy. In fact, the calculated barrier (via transition structure **23**) is only 1 kJ mol^{-1}. Hence, it is unlikely that either CH_2COH^{3+} (**13**) or $\overline{CHOHCH}^{3+}$ (**15**) will be experimentally observable.

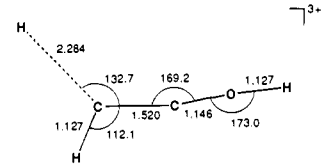

20 (C_s)

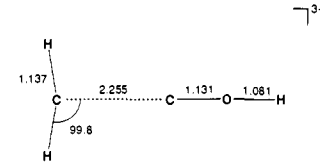

21 (C_{2v})

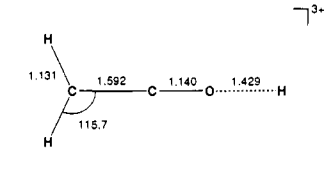

22 (C_{2v})

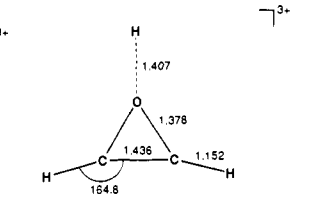

23 (C_s)

Concluding Remarks

Several important points emerge from this study:

(1) The calculated equilibrium geometries (MP2/6-31G* and MP2/6-311G*) and relative energies (MP4/6-311G** and MP4/6-311G(2d,2p)) for the cyclic [cyclopropenyl (**1**)] and open-chain [propargyl (**2**)] structures of $C_3H_3^+$ are in very good agreement with experimental values. The rearrangement reaction of **2** to **1** is predicted to have a large activation barrier of 408 kJ mol^{-1}.

(2) In contrast to the $C_3H_3^+$ system, which favors a cyclic structure, the multiply charged analogues prefer open-chain forms. This difference in behavior is attributed to the strong coulomb repulsion (between positively charged hydrogens) in the multiply charged species.

(3) The global minimum on the $C_2H_3N^{2+}$ potential energy surface corresponds to the open-chain CH_2NCH^{2+} structure (**6**). The cyclic isomer, $\overline{CHNHCH}^{2+}$ (**9**), lies 35 kJ mol^{-1} higher in energy than the open form. Both **6** and **9** are predicted to be thermodynamically stable with respect to proton losses and should be readily observable. The calculated heats of formation for **6** and **9** are 2630 and 2665 kJ mol^{-1}, respectively.

(4) The open-chain NH_2NCH^{3+} structure (**10**) is the most stable $CH_3N_2^{3+}$ ion. The cyclic structure, $\overline{NHCHNH}^{3+}$ (**12**), lies close in energy (39 kJ mol^{-1} above **10**). Both ions (**10** and **12**) are characterized by highly exothermic fragmentation reactions. However, significant barriers are found to be associated with these reactions. Hence, NH_2NCH^{3+} and $\overline{NHCHNH}^{3+}$ are predicted to be potentially observable in the gas phase.

(5) As for $C_2H_3N^{2+}$ and $CH_3N_2^{3+}$, $C_2H_3O^{3+}$ also favors an open-chain structure, CH_2CCOH^{3+} (**13**). In this case, however, the cyclic structure, $\overline{CHOHCH}^{3+}$ (**15**), is significantly higher in energy (234 kJ mol^{-1} above **13**). These two isomers (**13** and **15**)

are calculated to have very small barriers associated with deprotonation and, therefore, are unlikely to be observable in the gas phase.

(6) No stable equilibrium structures were found for the tetracation analogues of $C_3H_3^+$, namely $H_3N_3^{4+}$, CH_3NO^{4+}, and $C_2H_3F^{4+}$.

Acknowledgment. We are grateful for the generous allocation of computer time on the Fujitsu FACOM VP-100 of the Australian National University Supercomputer Facility.

Influence of Heavy Atoms on the Deactivation of Singlet Oxygen ($^1\Delta_g$) in Solution

Reinhard Schmidt

Contribution from the Institut für Physikalische Chemie, Universität Frankfurt, Niederurseler Hang, D 6000 Frankfurt/Main, FRG. *Received September 12, 1988*

Abstract: A very sensitive infrared emission spectrometer and very low excitation powers were used to determine $^1O_2$ lifetimes (τ_Δ) directly from phosphorescence decays in various chlorine-, bromine-, or iodine-substituted perfluorinated solvents. Laser-pulsed excitation was employed for measurement of τ_Δ in various halogen-substituted benzenes and perdeuterobenzenes. From the data the influence of heavy-atom-substituted solvents on radiationless $^1O_2$ deactivation has been studied. Radiationless deactivation occurs by collisional E → V energy transfer from $^1O_2$ to single oscillators X–Y of the solvent molecule. If the heavy atom is part of the energy accepting oscillator X–Y, a strong increase of intercombination probability is observed correlating with the square of the spin–orbit interaction energy of the heavy atom. If the heavy atom is not part of X–Y, only a very weak external heavy-atom effect on the collisional $^1O_2$ deactivation takes place. A model describing collisional $^1O_2$ deactivation by solvent molecules yields τ_Δ values for a large variety of solvents, which excellently agree with experimental data over the entire range of 4.5 orders of magnitude.

The lifetime (τ_Δ) of singlet oxygen ($^1\Delta_g$, $^1O_2$) in solution is extremely sensitive to the nature of the solvent and varies over a wide range from 4 to 100 000 μs.[1,2] Deactivation of $^1O_2$ in most solvents is largely radiationless by collisional electronic to vibrational (E → V) energy transfer from $^1O_2$ to a single oscillator of a solvent molecule.[2,3] The most probable energy-accepting oscillator of the solvent molecule is that terminal atom pair with the highest fundamental vibrational energy.[2]

Radiative deactivation of $^1O_2$ by phosphorescence emission at 1275 nm plays only a minor role since the emissive $^1\Delta_g \rightarrow {}^3\Sigma_g^-$ transition is highly forbidden. A very low phosphorescence quantum yield of $Q_P = 4.7 \times 10^{-5}$ in benzene has recently been calculated by us from corrected emission spectra, using an infrared luminescence spectrometer with known spectral sensitivity.[4] Q_P depends like τ_Δ very strongly on solvent. In the weakly deactivating solvent freon-113 ($C_2F_3Cl_3$), two independent methods gave $Q_P = 0.15$, a maximum value.[4,5]

Radiationless deactivation of $^1O_2$ by $^1\Delta_g \rightarrow {}^3\Sigma_g^-$ intersystem crossing (isc) is expected to be of no importance in solution. The Franck–Condon (FC) factor of the $^1\Delta_g$ ($v = 0$) → $^3\Sigma_g^-$ ($v = 5$) transition can be extrapolated from literature data to be on the order of 10^{-13}.[2,6] However, this transition is still exergonic by 337 cm^{-1}, and thus this estimate appears even to be an upper limit value for the FC factor of isoenergetic isc.[7] $^1O_2$ lifetimes of about 10 s have been determined in emission experiments at reduced pressure in the gas phase.[8] Since these values are 100 times larger than the maximum value of τ_Δ in solution, it is clear that even in weakly deactivating solvents isc does not contribute to the deactivation of $^1O_2$.

As deactivation of $^1O_2$ demands a change of multiplicity, an acceleration due to spin–orbit coupling can be expected under the influence of heavy atoms. However, preliminary results of Hurst and Schuster[3] indicate only a small and $^1O_2$ lifetime-dependent heavy-atom effect on τ_Δ. To get more insight into this puzzling problem, we determined lifetimes of $^1O_2$ for a variety of highly purified halogenated solvents of very different deactivating power using low excitation energies. The evaluation and discussion of the results in context with data obtained already earlier in this laboratory actually reveals a subtle but strong effect of heavy atoms on the radiationless $^1O_2$ deactivation process.

Experimental Section

The solvents used were benzene (C_6H_6), spectroscopic grade from Merck, and fluorobenzene (C_6H_5F, 99%), chlorobenzene (C_6H_5Cl, 99+%), bromobenzene (C_6H_5Br, 99+%), iodobenzene (C_6H_5I, 99%), benzene-d_6 (C_6D_6, 99.5%), bromobenzene-d_5 (C_6D_5Br, 99+%), hexafluorobenzene (C_6F_6, 99%), chloropentafluorobenzene (C_6F_5Cl, 95%), bromopentafluorobenzene (C_6F_5Br, 99%), iodopentafluorobenzene (C_6F_5I, 99%), fluorotrichloromethane ($CFCl_3$, 99+%), dibromotetrafluoroethane ($C_2F_4Br_2$), and perfluorohexyliodide ($C_6F_{13}I$, 99%) from Aldrich. All solvents were purified by column chromatography with neutral Al_2O_3 (Woelm). With C_6F_5Cl, which was originally only of 95% purity, this procedure was performed three times, 5,10,15,20-Tetraphenylporphine (TPP) (Aldrich gold label), methylene blue (MB) (Fluka, puriss.), and D_2O (Merck, Sharp, & Dohme, 99.96%) were used without further purification. H_2O was distilled twice. Rubicene (RUB) was prepared by the procedure described by Clar.[9] All solutions were air saturated, and the experimental temperature was about 22 °C.

The infrared luminescence spectrometer, which could be modified either to record spectra or to determine $^1O_2$ lifetimes ($\tau_\Delta \geq 7$ ms), has been described.[2] In lifetime measurements the excitation pulses were produced from a stationary excitation source by means of a chopper. Pulse energy amounted to <20 μJ, and pulse power, to <2 mW. The excitation wavelengths for the sensitizers TPP, RUB, and MB were chosen in each experiment to be outside the absorption range of the purified solvents. In order to prevent quenching of $^1O_2$ the sensitizers were used in very low concentrations in the weakly deactivating solvents, i.e. 0.6×10^{-6}–6×10^{-6} M depending on sensitizer and solvent. For

(1) Rodgers, M. A. J. *J. Am. Chem. Soc.* **1983**, *105*, 6201–6205.
(2) Schmidt, R.; Brauer, H.-D. *J. Am. Chem. Soc.* **1987**, *109*, 6976–6981.
(3) Hurst, J. R.; Schuster, G. B. *J. Am. Chem. Soc.* **1983**, *105*, 5756–5760.
(4) Schmidt, R. *Chem. Phys. Lett.* **1988**, *151*, 369–374.
(5) Schmidt, R.; Seikel, K.; Brauer, H.-D. *J. Phys. Chem.* **1989**, *93*, 4507–4511.
(6) Halmann, M.; Laulicht, I. *J. Chem. Phys.* **1965**, *43*, 438–448.
(7) Herzberg, G. *Spectra of Diatomic Molecules*; Van Nostrand Reinhold: New York, 1950; p 560.
(8) Clark, I. D.; Wayne, R. P. *Proc. R. Soc. London, A* **1969**, *314*, 111.
(9) Clar, E.; Willicks, W. *J. Chem. Soc.* **1958**, 942–946.

0002-7863/89/1511-6983$01.50/0